

On the Distribution of the Sum of Double-Nakagami- m Random Vectors and Application in Reconfigurable Intelligent Surfaces

Sotiris A. Tegos, *Student Member, IEEE*, Dimitrios Tyrovolas, *Student Member, IEEE*,
Panagiotis D. Diamantoulakis, *Senior Member, IEEE*, and George K. Karagiannidis, *Fellow, IEEE*

Abstract—Reconfigurable intelligent surfaces (RISs) intend to improve significantly the performance of future wireless networks, by controlling the wireless propagation medium through elements that can shift the phase of the reflected signals. Although ideally the signals reflected from a RIS are added coherently at the receiver, this is very challenging in practice due to the requirement for perfect channel state information (CSI) at the RIS and phase control. To facilitate the performance analysis of more practical RIS-assisted systems, first, we present novel closed-form expressions for the probability density function, the cumulative distribution function, the moments, and the characteristic function of the distribution of the sum of double-Nakagami- m random vectors, whose amplitudes follow the double-Nakagami- m distribution, i.e., the distribution of the product of two random variables following the Nakagami- m distribution, and phases are circular uniformly distributed. We also consider a special case of this distribution, namely the distribution of the sum of Rayleigh-Nakagami- m random vectors. Then, we exploit these expressions to investigate the performance of the RIS-assisted composite channel, assuming that the two links undergo Nakagami- m fading and the equivalent phase follows the uniform distribution, which corresponds to the case where CSI is not available at the RIS and leads to a lower bound of the performance of a system with CSI. Closed-form expressions for the outage probability, the average received signal-to-noise ratio, the ergodic capacity, the bit error probability, the amount of fading, and the channel quality estimation index are provided to evaluate the performance of the considered system. These metrics are also derived for the practical special case where one of the two links undergoes Rayleigh fading.

Index Terms—reconfigurable intelligent surfaces, phase estimation errors, double-Nakagami- m fading

I. INTRODUCTION

NOWADAYS, the need for higher data rate grows exponentially as the number of smart devices demanding ultra reliable and low latency connection to mobile networks keeps increasing following Edholm's law [1]. Fifth generation (5G) wireless networks enable massive communications and are able to serve the users with a wide range of services such as autonomous vehicles, virtual reality applications, industrial internet of things (IIoT), etc. The upcoming advent of the sixth generation (6G) wireless networks requires ultra low latency, coverage extension, improved throughput and security leading to communications on higher frequency bands like millimeter

wave (mmWave) and wireless optical communications [2], [3]. The main obstacles of communications in these bands are the sensitivity to blockage due to higher atmospheric attenuation, thus severe path loss and limited coverage. One solution for the aforementioned problem is the denser deployment of base stations (BSs) which can fill coverage holes, reduce the path loss, and facilitate higher rates, but with a higher cost and power consumption. To this end, the development of a smart radio environment (SRE) [4] is considered as an operational alternative due to their ability to provide large spectrum bandwidth with lower cost compared to the denser deployment of BSs.

Until recently, the propagation medium in the field of wireless communications has been perceived as a randomly behaving entity between the communicating systems, which negatively affects the quality of the received signal, due to the uncontrollable interactions (reflections, scattering, etc.) of the transmitted radio waves with the surrounding objects [5]. However, in the future SREs, the wireless propagation is envisioned to be controllable and the information to be processed through the transmission. This is facilitated by the ability of SREs to provide future wireless networks with uninterrupted wireless connectivity, using reconfigurable intelligent surfaces (RISs). A RIS can be thought as an inexpensive smart material sheet, which can be deployed easily and is capable of shaping the radio waves impinging upon it in a desired way [6]. Hence, RISs offer a new method for passive beamforming and are nominated to assist in low-cost and power-efficient information transferring. They can also extend the network coverage by overcoming the non-line-of-sight (NLoS) links between the terminals and improve the severe path loss in extremely high frequencies.

A. Motivation

A RIS can be abstracted into an array of low-cost tunable passive reflecting elements, that induce adjustable phase shifts on the reflected signals. Most of the studies assume continuous phase configuration and perfect knowledge of the phase shifts induced by the wireless channel through the RIS. Specifically, the authors of [7] provided a comprehensive theoretical framework for the performance characterization of RIS-assisted communications in different propagation scenarios. They derived closed-form expressions for the outage probability and the ergodic capacity for different fading environments,

The authors are with the Wireless Communications and Information Processing (WCIP) Group, Electrical & Computer Engineering Dept., Aristotle University of Thessaloniki, 54 124, Thessaloniki, Greece (e-mails: {tegotosi,tyrovolas,padiaman,geokarag}@auth.gr).

assuming perfect phase estimation. In [8], a RIS-assisted system where a RIS is deployed to assist the communication between a multi-antenna BS and multiple single-antenna users is investigated and the total transmit power is minimized. As far as the fading channel is concerned, Rayleigh fading model is commonly chosen for performance analysis [5], [9]–[11] which may not be a legit choice for a practical RIS-assisted communication scenario due to the fact that RISs are carefully deployed to leverage line-of-sight (LoS) links between the terminals.

In order to achieve perfect phase estimation, the RIS requires channel state information (CSI). However, due to the fact that RISs are considered as nearly passive circuits, channel estimation units cannot be integrated into them, thus in practical RIS-assisted systems perfect phase estimation is not possible. In [12], in a RIS-assisted system without CSI, the beamforming at the BS and IRS is optimized with particle swarm optimization. In [13], the communication through a RIS whose phase errors follow the Von Mises distribution, was investigated. This setup could represent imperfect phase estimation, quantized reflection phases, or both of them. The composite channel was proved to be equivalent to a point-to-point Nakagami- m fading channel by using the central limit theorem (CLT). However, the CLT does not provide accurate results for a RIS with small number of elements. Moreover, in recent studies, unified mathematical models for the outage probability and the ergodic capacity of RIS-assisted communication scenarios have been derived [14]. The authors of [15] derived the probability density function (PDF) of the channel fading coefficients, between a BS, a RIS and a single-antenna user, where the channel amplitude is assumed to follow a double-Nakagami- m distribution, and the phase estimation errors follow the Von Mises distribution. However, a closed-form expression for the PDF was not provided. In [16], the impact of quantized phase shifts on the performance of RIS-assisted communications was investigated. Specifically, BEP was calculated by leveraging the characteristic function estimated through the Gauss-Chebyshev quadrature approximation. Finally, in [11], a Rayleigh fading channel was considered where a multi-antenna transmitter communicates with a multi-antenna receiver through a RIS whose elements were impaired by phase noise and the performance of the considered system was analyzed by using Gamma approximation for large number of elements. Concluding the state-of-the-art, to the best of the authors' knowledge, a closed-form analysis of the Nakagami- m RIS communication channel without CSI at the RIS or with phase errors has not yet been presented in the open literature.

B. Contribution

To this end, in this paper, we investigate a practical RIS-assisted system where CSI is not available at the RIS, by utilizing the distribution of the sum of double-Nakagami- m random vectors, and provide exact closed-form expressions for its performance metrics. Specifically, the contributions of this work are listed below:

- We investigate the distribution of the sum of double-Nakagami- m random vectors, whose amplitudes follow the

double-Nakagami- m distribution, i.e., the distribution of the product of two random variables (RVs) following the Nakagami- m distribution, and phases are circular uniformly distributed, and provide exact closed form expressions for its statistical properties, i.e., the PDF, the cumulative distribution function (CDF), the moments and the characteristic function. These statistical properties are also derived for the distribution of the sum of Rayleigh-Nakagami- m random vectors which is a special case of the former distribution, where the amplitudes of the vectors follow the distribution of the product of a RV following the Rayleigh distribution and one following the Nakagami- m distribution.

- We utilize the derived expressions to investigate a practical RIS-assisted system where Nakagami- m fading channel is assumed both between the BS and the RIS and between the RIS and the user. Also, the equivalent phase is assumed to follow the uniform distribution, which corresponds to the case where CSI is not available at the RIS and leads to a lower bound of the performance of a system with CSI. We extract useful metrics to investigate the performance of the considered system, such as the outage probability, the average received signal-to-noise ratio (SNR), which is proved to be proportional to the number of elements, the ergodic capacity, the BEP for both binary and M -ary modulations, the amount of fading (AoF) and the channel quality estimation index (CQEI). These metrics are also provided for the practical special case where one of the links undergoes Rayleigh fading, where the derived expressions are significantly simplified.

C. Structure

The rest of the paper is organized as follows: In Section II, the statistical properties of the distribution of the sum of double-Nakagami- m random vectors and the distribution of the sum of Rayleigh-Nakagami- m random vectors are provided. In Section III, a RIS-assisted system is investigated, useful performance metrics are provided and numerical results are provided to illustrate the performance of the considered system. Finally, closing remarks and discussion are provided in Section IV.

II. THE DISTRIBUTION OF THE SUM OF DOUBLE-NAKAGAMI- m RANDOM VECTORS

We consider N double-Nakagami- m random vectors, X_k , $k \in \{1, N\}$, with amplitudes $|h_k|$ and phases θ_k , i.e.,

$$X_k = |h_k|e^{j\theta_k}. \quad (1)$$

The amplitudes $|h_k|$ are independent and identically distributed RVs, which follow the double-Nakagami- m distribution with parameters m_1 , m_2 , Ω_1 and Ω_2 , i.e., the distribution of the product of two RVs following the Nakagami- m distribution, whose PDF is given by [17]

$$f_{h_k}(z) = \frac{4z^{m_1+m_2-1}}{\Gamma(m_1)\Gamma(m_2)} \left(\frac{m_1 m_2}{\Omega_1 \Omega_2} \right)^{\frac{m_1+m_2}{2}} \times K_{m_1-m_2} \left(2z \sqrt{\frac{m_1 m_2}{\Omega_1 \Omega_2}} \right), \quad (2)$$

where $\Gamma(\cdot)$ is the Gamma function [18]. Moreover, the phases θ_k are uniformly distributed in $[0, 2\pi]$.

Next, we define the vector H as

$$H = \sum_{k=1}^N X_k. \quad (3)$$

Theorem 1: The PDF of $|H|$ can be expressed in closed-form as

$$f_{|H|}(r) = \sum_{k_1=0}^{m_1-1} \dots \sum_{k_N=0}^{m_1-1} \prod_{i=1}^N \frac{(m_2)_{m_1-1-k_i} (1-m_2)_{k_i}}{(m_1-1-k_i)! k_i!} \times \frac{4 \left(\frac{m_1 m_2}{\Omega_1 \Omega_2} \right)^{\frac{u+1}{2}}}{(u-1)!} r^u K_{u-1} \left(2 \sqrt{\frac{m_1 m_2}{\Omega_1 \Omega_2}} r \right), \quad (4)$$

where $u = N(m_1 + m_2 - 1) - \sum_{i=1}^N k_i$, $K_v(\cdot)$ is the v -th order modified Bessel function of the second kind [18], $(n)_k$ is the Pochhammer symbol and $k!$ is the factorial of k .

Proof: The proof is provided in Appendix A. ■

It should be highlighted that m_1 and m_2 are used interchangeably. In the following proposition, we present the PDF for a special case, where the amplitudes of the vectors follow the distribution of the product of a RV following the Rayleigh distribution and one following the Nakagami- m distribution, i.e., the distribution of the sum of Rayleigh-Nakagami- m random vectors.

Proposition 1: The PDF of $|H|$, when H follows the distribution of the sum of Rayleigh-Nakagami- m random vectors, can be expressed in closed-form as

$$f_{|H|}(r) = \frac{4 \left(\frac{m}{\Omega_1 \Omega_2} \right)^{\frac{Nm+1}{2}}}{(Nm-1)!} r^{Nm} K_{Nm-1} \left(2 \sqrt{\frac{m}{\Omega_1 \Omega_2}} r \right). \quad (5)$$

Proof: Without loss of generality, since in (4) m_1 and m_2 are used interchangeably, we set $m_1 = 1$ and $m_2 = m$ and (5) is derived. ■

Remark 1: The distribution of the sum of Rayleigh-Nakagami- m random vectors is a double-Nakagami- m distribution with PDF given by (2) where $m_1 = 1$, $m_2 = Nm$, and replacing Ω_2 with $N\Omega_2$.

In the following theorem, the CDF of the amplitude of the sum of double-Nakagami- m random vectors is derived in closed-form.

Theorem 2: The CDF of $|H|$ can be expressed as

$$F_{|H|}(r) = \sum_{k_1=0}^{m_1-1} \dots \sum_{k_N=0}^{m_1-1} \prod_{i=1}^N \frac{(m_2)_{m_1-1-k_i} (1-m_2)_{k_i}}{(m_1-1-k_i)! k_i!} \times \left(1 - \frac{2}{(u-1)!} \left(\sqrt{\frac{m_1 m_2}{\Omega_1 \Omega_2}} r \right)^u K_u \left(2 \sqrt{\frac{m_1 m_2}{\Omega_1 \Omega_2}} r \right) \right). \quad (6)$$

Proof: The CDF of $|H|$ is defined as

$$F_{|H|}(r) = \int_0^r f_{|H|}(x) dx. \quad (7)$$

Also, from [19, 03.04.21.0010.01], it stands that

$$\int x^u K_{u-1}(x) dx = -x^u K_u(x). \quad (8)$$

Since $x^u K_u(x)$ is not defined in 0, we utilize the following limit, which we prove in Appendix B,

$$\lim_{x \rightarrow 0} x^v K_v(x) = 2^{v-1} (v-1)!, \quad v \in \mathbb{Z}, v > 0 \quad (9)$$

and after some algebraic manipulations, (6) is derived. ■

Next, we provide the CDF of $|H|$ for the considered special case.

Proposition 2: The CDF of $|H|$, when H follows the distribution of the sum of Rayleigh-Nakagami- m random vectors, can be expressed in closed-form as

$$F_{|H|}(r) = 1 - \frac{2}{(Nm-1)!} \left(\sqrt{\frac{m}{\Omega_1 \Omega_2}} r \right)^{Nm} \times K_{Nm} \left(2 \sqrt{\frac{m}{\Omega_1 \Omega_2}} r \right). \quad (10)$$

Proof: Setting $m_1 = 1$ and $m_2 = m$ in (6), (10) is derived. ■

Next, we derive closed-form expression for the moments of the amplitude of the sum of double-Nakagami- m random vectors.

Theorem 3: The n -th moment of $|H|$ can be formulated as

$$\mu^n = \left(\frac{\Omega_1 \Omega_2}{m_1 m_2} \right)^{\frac{n}{2}} \sum_{k_1=0}^{m_1-1} \dots \sum_{k_N=0}^{m_1-1} \prod_{i=1}^N \frac{(m_2)_{m_1-1-k_i} (1-m_2)_{k_i}}{(m_1-1-k_i)! k_i!} \frac{\Gamma\left(\frac{n}{2}+1\right) \Gamma\left(\frac{n}{2}+u\right)}{\Gamma(u)}. \quad (11)$$

Proof: The n -th moment of $|H|$ is defined as

$$\mu^n = \int_0^\infty x^n f_{|H|}(x) dx. \quad (12)$$

Using [18, 6.561/16] and after some algebraic manipulations, (11) is derived. ■

Considering the even moments, the l -th moment of $|H|$ with $l = 2n$ can be simplified as

$$\mu^l = \left(\frac{\Omega_1 \Omega_2}{m_1 m_2} \right)^l \sum_{k_1=0}^{m_1-1} \dots \sum_{k_N=0}^{m_1-1} \prod_{i=1}^N \frac{(m_2)_{m_1-1-k_i} (1-m_2)_{k_i}}{(m_1-1-k_i)! k_i!} l!(u)_l. \quad (13)$$

In the following proposition, the moments of the considered distribution are derived for the special case.

Proposition 3: The n -th moment of $|H|$, when H follows the distribution of the sum of Rayleigh-Nakagami- m random vectors, can be expressed in closed-form as

$$\mu^n = \left(\frac{\Omega_1 \Omega_2}{m} \right)^{\frac{n}{2}} \frac{\Gamma\left(\frac{n}{2}+1\right) \Gamma\left(\frac{n}{2}+Nm\right)}{\Gamma(Nm)}. \quad (14)$$

Proof: Setting $m_1 = 1$ and $m_2 = m$ in (11), (14) is derived. ■

Considering the even moments for the special case, the l -th moment of $|H|$ can be simplified as

$$\mu^l = \left(\frac{\Omega_1 \Omega_2}{m} \right)^l l!(Nm)_l. \quad (15)$$

In the following theorem, we derive the characteristic function of the amplitude of the sum of double-Nakagami- m random vectors.

Theorem 4: The characteristic function of $|H|$ can be expressed in closed form as

$$\begin{aligned} \varphi_{|H|}(t) &= \sum_{k_1=0}^{m_1-1} \dots \sum_{k_N=0}^{m_1-1} \prod_{i=1}^N \frac{(m_2)_{m_1-1-k_i} (1-m_2)_{k_i}}{(m_1-1-k_i)! k_i!} \\ &\times \left(\frac{m_1 m_2}{\Omega_1 \Omega_2} \right)^u \left(\frac{2\sqrt{m_1 m_2}}{\sqrt{\Omega_1 \Omega_2}} - jt \right)^{-2u} \frac{2^{4u}}{1+2u} \\ &\times {}_2F_1 \left(2u, u - \frac{1}{2}, u + \frac{3}{2}, \frac{jt\sqrt{\Omega_1 \Omega_2} + 2\sqrt{m_1 m_2}}{jt\sqrt{\Omega_1 \Omega_2} - 2\sqrt{m_1 m_2}} \right), \end{aligned} \quad (16)$$

where $t \in \mathbb{R}$ and $j^2 = -1$.

Proof: The characteristic function of $|H|$ is defined as

$$\varphi_{|H|}(t) = \int_0^\infty e^{jtx} f_{|H|}(x) dx. \quad (17)$$

Using [18, 6.621/3] and after some algebraic manipulations, (16) is derived. ■

In the following proposition, the characteristic function is derived for the considered special case.

Proposition 4: The characteristic function of $|H|$, when H follows the distribution of the sum of Rayleigh-Nakagami- m random vectors, can be expressed in closed-form as

$$\begin{aligned} \varphi_{|H|}(t) &= \left(\frac{m_1 m_2}{\Omega_1 \Omega_2} \right)^{Nm} \left(\frac{2\sqrt{m_1 m_2}}{\sqrt{\Omega_1 \Omega_2}} - jt \right)^{-2Nm} \frac{2^{4Nm}}{1+2Nm} \\ &\times {}_2F_1 \left(2Nm, Nm - \frac{1}{2}, Nm + \frac{3}{2}, \frac{jt\sqrt{\Omega_1 \Omega_2} + 2\sqrt{m_1 m_2}}{jt\sqrt{\Omega_1 \Omega_2} - 2\sqrt{m_1 m_2}} \right). \end{aligned} \quad (18)$$

Proof: Setting $m_1 = 1$ and $m_2 = m$ in (16), (18) is derived. ■

III. APPLICATION IN RECONFIGURABLE INTELLIGENT SURFACES

In this section, we investigate a practical RIS-assisted system with phase errors and provide useful metrics to evaluate its performance.

A. System Model

We consider a communication system consisting of a BS with a single antenna, a RIS and a single user with a single antenna. The transmitted signal by the BS is reflected to the array, consisting of N reflecting elements, and then is received by the user. It is assumed that the direct link from the BS to the user is blocked by obstacles, such as buildings [7], which is a realistic assumption especially when high frequency bands are used.

The received signal, Y , in the user can be expressed as

$$Y = \sqrt{lp} \sum_{k=1}^N e^{j\phi_k} H_{1k} H_{2k} X + W, \quad (19)$$

where X and W denote the transmitted signal and the additive white Gaussian noise, respectively, and e is the basis of the

natural logarithm. The complex channel coefficients between the BS and the RIS and between the RIS and the user are denoted by H_{1k} and H_{2k} , respectively. Moreover, l , p , and ϕ_k denote the equivalent path loss, the transmitted power, and the phase adjustment performed by the RIS, respectively. It is assumed that $|H_{1k}|$ and $|H_{2k}|$ are RVs following the Nakagami- m distribution with shape parameters m_1 and m_2 , respectively, and spread parameters Ω_1 and Ω_2 , respectively, which are the same for all N elements [15].

The RIS attempts to cancel the phase introduced by the product of the two complex channel coefficients, H_{1k} and H_{2k} , with the use of the phase adjustment ϕ_k . Assuming that CSI is not available at the RIS, ϕ_k is uniformly distributed in $[0, 2\pi]$. Considering that $\arg(H_{1k})$ and $\arg(H_{2k})$, where $\arg(\cdot)$ denotes the argument of a complex number, are uniformly distributed in $[0, 2\pi]$ and the fact the sum of m RVs which follow the circular uniform distribution also follows the circular uniform distribution, $\theta_k = \phi_k + \arg(H_{1k}) + \arg(H_{2k})$ is uniformly distributed in $[0, 2\pi]$. Equivalently, considering a system with CSI, ϕ_k is chosen so that $\phi_k + \arg(H_{1k}) + \arg(H_{2k}) = 0$. However, in practical systems, the phase correction is not perfect resulting in residual phase error θ_k [13]. The phase error θ_k is frequently modeled as a RV following the Von Mises distribution with concentration parameter κ [13]. If $\kappa = 0$, the distribution of θ_k is uniform and for small values of κ the distribution is close to uniform. When $\kappa = 0$, the phase errors are equally probable, thus this case is the worst one and can be considered as a lower bound of the performance of a system with CSI. To this end, in this work, we assume that the equivalent phase θ_k is uniformly distributed in $[0, 2\pi]$, which corresponds to both previously mentioned cases. Therefore, the received signal in (19) can be expressed as

$$Y = \sqrt{lp} \sum_{k=1}^N e^{j\theta_k} |H_{1k}| |H_{2k}| X + W. \quad (20)$$

We define the composite channel coefficient H as

$$H = \sum_{k=1}^N e^{j\theta_k} |H_{1k}| |H_{2k}|. \quad (21)$$

Therefore, the PDF of the composite channel coefficient $|H|$ is given by (4).

B. Performance Evaluation

In this subsection, the performance of the considered system is evaluated in terms of the outage probability and the average received SNR.

Corollary 1: The outage probability can be obtained through (6) as

$$P_o = F_{|H|} \left(\sqrt{\frac{\gamma_{\text{thr}}}{l\gamma_t}} \right), \quad (22)$$

where γ_t denotes the transmitted SNR and γ_{thr} denotes the threshold which defines the outage.

If we consider the special case where one link follows the Nakagami- m distribution and the other link follows the Rayleigh distribution, the outage probability can be expressed using (10).

In the following proposition, the average received SNR is provided which is proved to be independent of m_1 and m_2 , thus it can be utilized for both considered cases.

Proposition 5: The average received SNR is given by

$$\mathbb{E}[\gamma_r] = lN\Omega_1\Omega_2\gamma_t. \quad (23)$$

Proof: The average received SNR can be obtained as

$$\mathbb{E}[\gamma_r] = l\mathbb{E}[|H|^2]\gamma_t, \quad (24)$$

where $\mathbb{E}[|H|^2]$ is the expected value of the channel gain which can be derived as the second moment in (11), i.e.,

$$\mathbb{E}[|H|^2] = \frac{\Omega_1\Omega_2}{m_1m_2} \sum_{k_1=0}^{m_1-1} \dots \sum_{k_N=0}^{m_1-1} \prod_{i=1}^N \frac{(m_2)_{m_1-1-k_i}(1-m_2)_{k_i}}{(m_1-1-k)!k_i!} u. \quad (25)$$

Using [19, 06.10.16.0005.01] and the fact that $(1)_n = n!$, $n \in \mathbb{Z}, n > 0$, it is proven that

$$\sum_{k_i=0}^{m_1-1} \frac{(m_2)_{m_1-1-k_i}(1-m_2)_{k_i}}{(m_1-1-k)!k_i!} = 1. \quad (26)$$

Moreover, using [19, 06.10.17.0002.02], it is proven that

$$k_i(1-m_2)_{k_i} = (1-m_2)((2-m_2)_{k_i} - (1-m_2)_{k_i}). \quad (27)$$

Using (26) and (27), it can be proven that

$$\sum_{k_i=0}^{m_1-1} \frac{k_i(m_2)_{m_1-1-k_i}(1-m_2)_{k_i}}{(m_1-1-k)!k_i!} = (1-m_2)(m_1-1). \quad (28)$$

Utilizing (26) and (28) and after some algebraic manipulations, (23) is derived. ■

Remark 2: It should be highlighted that the average received SNR is proportional to the number of elements N , since we consider that phase errors are uniformly distributed which leads to a lower bound in the performance of a system with CSI where there is no phase error and the average received SNR is proportional to N^2 [13].

Next, we provide the ergodic capacity of the considered system.

Proposition 6: The ergodic capacity can be expressed as

$$C = \frac{B}{\ln 2} \sum_{k_1=0}^{m_1-1} \dots \sum_{k_N=0}^{m_1-1} \prod_{i=1}^N \frac{(m_2)_{m_1-1-k_i}(1-m_2)_{k_i}}{(m_1-1-k)!k_i!} \times \frac{1}{(u-1)!} G_{3,1}^{1,3} \left(\frac{l\gamma_t\Omega_1\Omega_2}{m_1m_2} \middle| \begin{matrix} 1, 1, 1-u \\ 1 \end{matrix} \right), \quad (29)$$

where B denotes the bandwidth of the fading channel.

Proof: The ergodic capacity is calculated as the average capacity and is given by

$$C = B \int_0^\infty \log_2(1 + l\gamma_t r^2) f_{|H|}(r) dr. \quad (30)$$

TABLE I
VALUES OF a AND b IN (33) FOR DIFFERENT BINARY MODULATIONS.

Modulation	a	b
BPSK	1	$\frac{1}{2}$
DBPSK	1	1
BFSK	$\frac{1}{2}$	$\frac{1}{2}$
NBFSK	$\frac{1}{2}$	1

Transforming $\ln(1+x)$ into Meijer's G-function [19, 01.04.26.0002.01] and using [19, 03.04.26.0037.01] and [20], the ergodic capacity can be evaluated as

$$C = \frac{B}{\ln 2} \sum_{k_1=0}^{m_1-1} \dots \sum_{k_N=0}^{m_1-1} \prod_{i=1}^N \frac{(m_2)_{m_1-1-k_i}(1-m_2)_{k_i}}{(m_1-1-k)!k_i!} \times \frac{1}{(u-1)!} G_{4,2}^{1,4} \left(\frac{l\gamma_t\Omega_1\Omega_2}{m_1m_2} \middle| \begin{matrix} 1, 1, 1-u, 0 \\ 1, 0 \end{matrix} \right). \quad (31)$$

Using [19, 07.34.04.0002.01] and [19, 07.34.03.0001.01], the Meijer's G-function can be simplified and (29) is derived, which completes the proof. ■

For the considered special case, the ergodic capacity can be expressed as

$$C = \frac{B}{\ln 2(Nm-1)!} G_{3,1}^{1,3} \left(\frac{l\gamma_t\Omega_1\Omega_2}{m} \middle| \begin{matrix} 1, 1, 1-Nm \\ 1 \end{matrix} \right). \quad (32)$$

Next, we provide the BEP of the RIS-assisted system for binary modulations, i.e., binary phase-shift keying (BPSK), differential binary phase-shift keying (DBPSK), binary frequency-shift keying (BFSK) and noncoherent binary frequency-shift keying (NBFSK). In this case, the BEP is given by [21]

$$P_e^b(H) = \frac{1}{2\Gamma(b)} \Gamma(b, a|H|^2\gamma_t), \quad (33)$$

where a and b are modulation-dependent parameters which are presented in Table I and $\Gamma(\cdot, \cdot)$ is the upper incomplete Gamma function [18].

Proposition 7: The BEP for binary modulations is given by

$$P_e^b = \frac{1}{2\Gamma(b)} \sum_{k_1=0}^{m_1-1} \dots \sum_{k_N=0}^{m_1-1} \prod_{i=1}^N \frac{(m_2)_{m_1-1-k_i}(1-m_2)_{k_i}}{(m_1-1-k)!k_i!} \times \frac{1}{(u-1)!} G_{3,2}^{2,2} \left(\frac{al\gamma_t\Omega_1\Omega_2}{m_1m_2} \middle| \begin{matrix} 1-u, 0, 1 \\ 0, b \end{matrix} \right). \quad (34)$$

Proof: Transforming $\Gamma(b, x)$ into Meijer's G-function [19, 06.06.26.0005.01] and using [19, 03.04.26.0037.01] and [20], (37) is derived, which completes the proof. ■

For the considered special case, the BEP for binary modulations can be obtained as

$$P_e^b = \frac{1}{2\Gamma(b)(Nm-1)!} G_{3,2}^{2,2} \left(\frac{al\gamma_t\Omega_1\Omega_2}{m} \middle| \begin{matrix} 1-Nm, 0, 1 \\ 0, b \end{matrix} \right). \quad (35)$$

Next, we provide the BEP of the RIS-assisted system considering M -ary modulations with $M \geq 4$, i.e., quadrature

TABLE II
VALUES OF τ_M , a_M AND b_k IN (36) FOR DIFFERENT MODULATIONS WITH $M \geq 4$.

Modulation	τ_M	a_M	b_k
M -QAM	$\frac{\sqrt{M}}{2}$	$\frac{2}{\log_2 M} \left(1 - \frac{1}{\sqrt{M}}\right)$	$\frac{3 \log_2 M}{2(M-1)} (2k-1)^2$
M -PSK	$\max\left(\frac{M}{4}, 1\right)$	$\frac{1}{\max(\log_2 M, 2)}$	$\log_2 M \sin^2\left(\frac{2k-1}{M}\pi\right)$

amplitude modulation (QAM) and PSK. In this case, considering that Gray mapping is used, the BEP is given by [22]

$$P_e(H) = a_M \sum_{k=1}^{\tau_M} \operatorname{erfc}\left(\sqrt{b_k l \gamma_t} |H|\right), \quad (36)$$

where a_M , τ_M and b_k are modulation-dependent parameters which are presented in Table II.

Proposition 8: The BEP for M -ary modulations can be expressed as

$$P_e = \frac{1}{\sqrt{\pi}} \sum_{k=1}^{\tau_M} \sum_{k_1=0}^{m_1-1} \dots \sum_{k_N=0}^{m_1-1} \prod_{i=1}^N \frac{(m_2)_{m_1-1-k_i} (1-m_2)_{k_i}}{(m_1-1-k_i)! k_i!} \\ \times \frac{1}{(u-1)!} G_{3,2}^{2,2} \left(\frac{b_k l \gamma_t \Omega_1 \Omega_2}{m_1 m_2} \middle| \begin{matrix} 1-u, 0, 1 \\ 0, \frac{1}{2} \end{matrix} \right). \quad (37)$$

Proof: Transforming $\operatorname{erfc}(x)$ into Meijer's G-function [19, 06.06.26.0005.01] and using [19, 03.04.26.0037.01] and [20], (37) is derived, which completes the proof. ■

For the considered special case, the BEP for M -ary modulations can be obtained as

$$P_e = \frac{1}{\sqrt{\pi} (Nm-1)!} \sum_{k=1}^{\tau_M} G_{3,2}^{2,2} \left(\frac{b_k l \gamma_t \Omega_1 \Omega_2}{m} \middle| \begin{matrix} 1-Nm, 0, 1 \\ 0, \frac{1}{2} \end{matrix} \right). \quad (38)$$

Next, we present the AoF, a useful performance metric for the analysis of wireless communication systems which expresses the severity of the fading channel and is defined as the ratio of the variance to the square average of the instantaneous received SNR, i.e., [23], [24]

$$\text{AoF} = \frac{\mathbb{E}[\gamma_r^2] - (\mathbb{E}[\gamma_r])^2}{(\mathbb{E}[\gamma_r])^2}. \quad (39)$$

In the considered RIS-assisted system, the AoF is calculated in the following proposition

Proposition 9: The AoF is given by

$$\text{AoF} = 1 + \frac{1 + m_1 + m_2 - m_1 m_2}{Nm_1 m_2}. \quad (40)$$

Proof: The proof is provided in Appendix C. ■

For the considered special case, (40) can be further simplified as

$$\text{AoF} = \frac{2 + Nm}{Nm}. \quad (41)$$

Next, we provide another useful performance metric, the CQEI, which assesses the error performance of a communication system efficiently and is defined as the ratio of the variance to the cubed mean of the instantaneous received SNR, i.e., [25]

$$\text{CQEI} = \frac{\mathbb{E}[\gamma_r^2] - (\mathbb{E}[\gamma_r])^2}{(\mathbb{E}[\gamma_r])^3}. \quad (42)$$

In the following proposition, the CQEI is extracted.

Proposition 10: The CQEI can be expressed as

$$\text{CQEI} = \frac{1 + m_1 + m_2 + m_1 m_2 (N-1)}{N^2 m_1 m_2 \Omega_1 \Omega_2 l \gamma_t}. \quad (43)$$

Proof: Considering that (42) can be written as

$$\text{CQEI} = \frac{\text{AoF}}{\mathbb{E}[\gamma_r]}, \quad (44)$$

CQEI can be directly derived from (23) and (40). ■

For the considered special case, (43) can be further simplified as

$$\text{CQEI} = \frac{2 + Nm}{N^2 m \Omega_1 \Omega_2 l \gamma_t}. \quad (45)$$

C. Numerical Results and Discussion

In this subsection, we illustrate the performance of the considered system. Assuming that both the BS and the user are located at the far field region of the RIS, the equivalent path loss l is given by $l = l_1 l_2$, where l_1 and l_2 denote the path loss of the link between the BS and the RIS and the link between the RIS and the user, respectively. The path loss of each link is modeled as [8]

$$l_i = C_0 \left(\frac{d_i}{d_0} \right)^{-\alpha}, \quad (46)$$

where C_0 denotes the reference path loss at the reference distance d_0 , d_i , $i \in \{1, 2\}$ denotes the distance of the i -th link and α denotes the path loss exponent. We set $m_1 = 3$, $m_2 = 1$, $\Omega_1 = 1$ and $\Omega_2 = 1$, which corresponds to a scenario where there is a LoS link between the BS and the RIS and a NLoS link between the RIS and the user. This scenario is motivated by the mobility of the user and, thus, the difficulty of establishing a LoS link [11]. Moreover, we also examine the setup where $m_1 = 1$ and $m_2 = 1$ in order to illustrate a performance lower bound which represents a scenario where the RIS is randomly deployed, since there is no LoS link. For both path loss links, we set $C_0 = -30\text{dB}$, $d_0 = 1\text{m}$, and the path loss exponent for the BS-RIS link and the RIS-user link is set as $a_1 = 2.8$ and $a_2 = 2.2$, respectively [8]. Furthermore, unless stated otherwise, the transmitted SNR is 110dB and it is assumed that the sum of the two distances is constant, i.e., $d_1 + d_2 = d$ with $d = 30\text{m}$. It is also assumed that as the number of elements increases, the size of the RIS also increases due to the fact that the inter-distance between them remains unchanged.

Fig. 1 illustrates the impact of the ratio of the transmitted SNR to the outage threshold in the receiver and the number of elements of the RIS on the outage probability. In this figure, we set the distance between the BS and the RIS as $d_1 = 25\text{m}$ and the distance between the RIS and the user is set as $d_2 = 5\text{m}$.

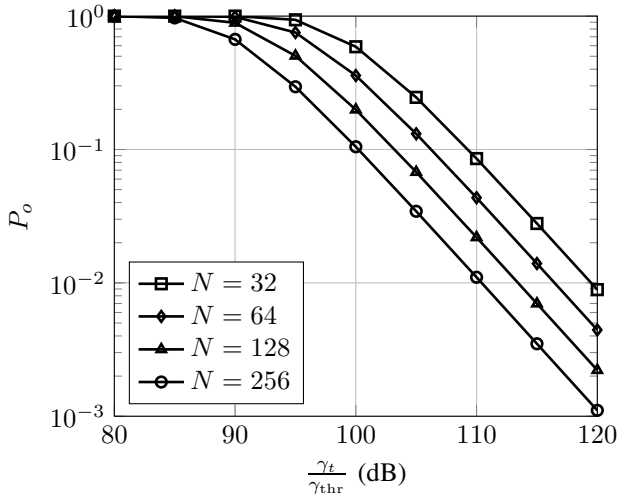


Fig. 1. Outage probability P_o versus $\frac{\gamma_t}{\gamma_{thr}}$.

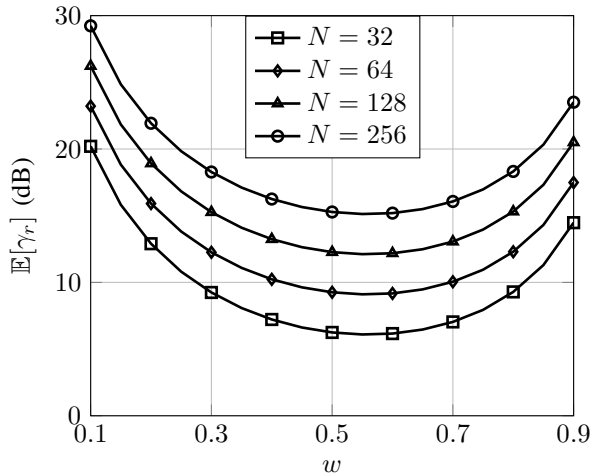


Fig. 2. Average received SNR versus w .

It is observed that as the number of elements increases the outage probability decreases, thus it is clear that the quality of service (QoS) can be improved by increasing the number of elements without increasing the power consumption of the transmitter. Specifically, it can be observed that by doubling the number of elements the same outage performance can be achieved with 3dB smaller transmitted SNR. However, in order to significantly improve the outage probability, the size of the RIS must be noticeably large, as in this way more electromagnetic power density will impinge upon the surface and, thus, more energy will be focused on the user leading to an increase of the received SNR.

In Fig. 2 and Fig. 4, we set $d_1 = wd$ and $d_2 = (1-w)d$, where $w \in [0.1, 0.9]$ to ensure that the terminals are located at the far field region, and the average received SNR and the BEP versus w are illustrated, respectively. For the BEP, the modulation is assumed to be either BPSK or 4-QAM with Gray mapping. It is observed that as the number of elements increases, both the average received SNR and the BEP increases at a certain distance. Moreover, it should be

highlighted that the placement of the RIS plays an important role and it becomes evident that it should be placed either close to the BS or close to the user, since the path losses are maximized when the RIS is placed in an intermediate point between the BS and the user. Also, the fact that the performance is slightly improved when the RIS is placed close to the BS is justified as the exponent a_1 is larger than a_2 .

Fig. 3 depicts the impact of the transmitted SNR on the ergodic capacity for different numbers of elements of the RIS. The distances of the two links are set as in Fig. 1. It is observed that high transmitted SNR values are required for successful information transmission. Moreover, increasing the number of elements leads to better ergodic capacity, since the average received SNR is proportional to the number of elements and the QoS can be improved by the enlargement of the RIS without consuming more power.

Fig. 5 illustrates how the AoF is affected by the number of elements of the RIS. As the number of elements increases, the AoF converges to 1. Especially for the case where $m_1 = 3$ and $m_2 = 2$ the amount of fading equals to 1 regardless of the number of elements. As the number of elements increases, due to the fact that phase shift of each element is a circular uniformly distributed RV, more non-coherent paths are created. Therefore, when a large RIS with arbitrary phase shift is deployed between two terminals, the AoF tends to 1, which coincides to the value of the AoF for a single Rayleigh channel. Moreover, as the AoF is hardly affected by the fading conditions for large number of elements, it follows that the fading conditions have limited impact on the performance of the considered system. It should be highlighted that as m_1 and m_2 are used interchangeably, the AoF is the same for the scenarios where the value of the shape parameters of both links is interchanged, e.g., $\text{AoF}_{3,1} = \text{AoF}_{1,3}$.

Fig. 6 depicts the behavior of the CQEI as the transmitted SNR increases. It should be highlighted that the performance improves as the CQEI decreases. It is clear that as the number of elements increases, the CQEI decreases without requiring larger transmitted SNR and as a consequence the system performance upgrades.

IV. CONCLUSIONS

In this work, we have utilized the distribution of the sum of double-Nakagami- m random vectors in a RIS-assisted system where the two links undergo Nakagami- m fading and imperfect phase correction is considered. Specifically, we have assumed that the equivalent phase follows the uniform distribution which corresponds to the case where CSI is not available at the RIS and leads to a lower bound of the performance of a system with CSI. We have derived closed-form expressions of useful metrics such as the outage probability, the average received SNR, the ergodic capacity, the BEP, the AoF and the CQEI. It has been proved that the average received SNR is proportional to the number of elements N , in contrast with the perfect phase shifting case where it is proportional to N^2 , and it can be observed that large number of elements is required in order to improve the system performance. Furthermore, we can enhance the system performance by deploying the RIS in

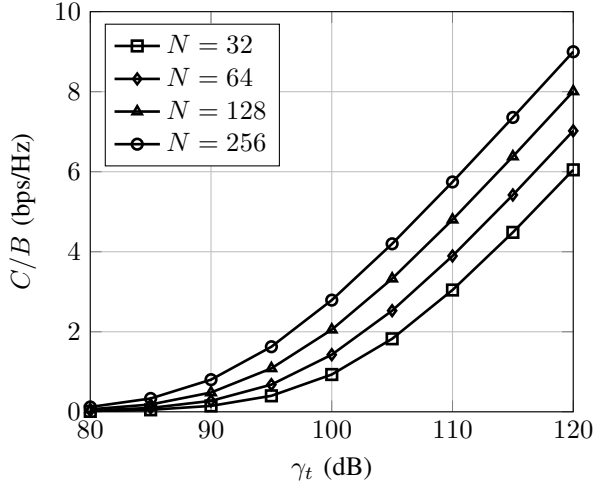


Fig. 3. Normalized ergodic capacity $\frac{C}{B}$ versus γ_t .

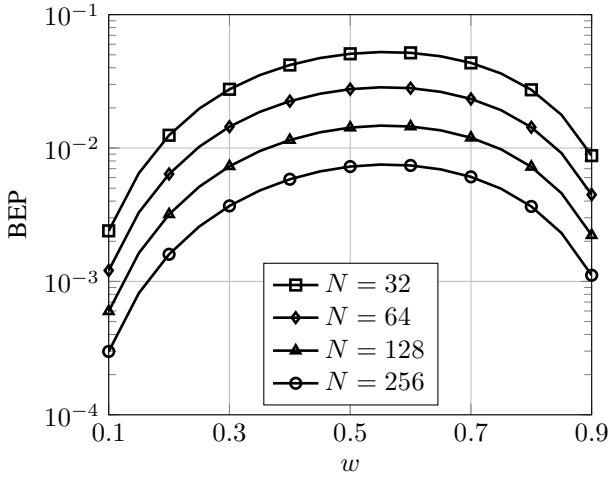


Fig. 4. BEP versus w for BPSK or 4-QAM modulation with Gray mapping.

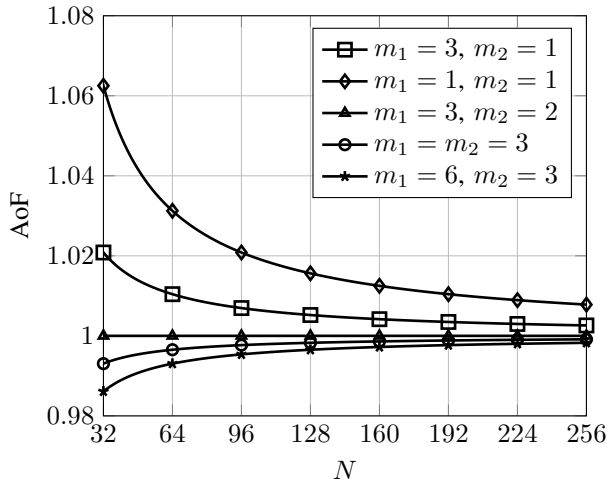


Fig. 5. AoF versus the number of elements N .

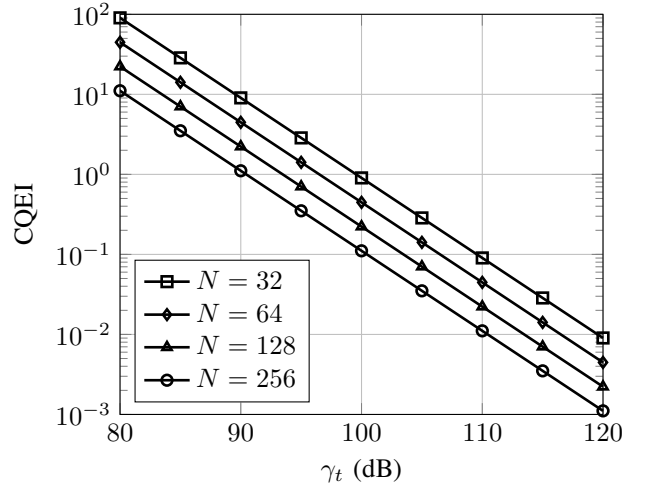


Fig. 6. CQEI versus γ_t .

the vicinity of the BS or the user. Finally, it has been illustrated that when a large RIS with arbitrary phase shift is deployed between two terminals, the AoF tends to 1, which coincides to the value of the AoF for a single Rayleigh channel.

APPENDIX A PROOF OF THEOREM 1

The PDF of $|H|$ is given by [26]

$$f_{|H|}(r) = r \int_0^\infty \rho J_0(r\rho) \Lambda(\rho) d\rho, \quad (47)$$

where $J_v(\cdot)$ is the v -th order Bessel function of the first kind [18] and $\Lambda(\rho)$ can be expressed as

$$\Lambda(\rho) = \mathbb{E}_{h_1 \dots h_N} \left[\prod_{i=1}^N J_0(h_i \rho) \right] = \prod_{i=1}^N \mathbb{E}_{h_i} [J_0(h_i \rho)]. \quad (48)$$

The expected value in (48) can be evaluated as

$$\mathbb{E}_{h_i} [J_0(h_i \rho)] = \int_0^\infty J_0(z\rho) f_h(z) dz. \quad (49)$$

Transforming the Bessel functions into Meijer's G-functions [19, 03.04.26.0037.01], [19, 03.01.26.0056.01] and using [20], (49) can be written as

$$\mathbb{E}_{h_i} [J_0(h_i \rho)] = \frac{1}{\Gamma(m_1)\Gamma(m_2)} \times G_{2,2}^{1,2} \left(\frac{\Omega_1 \Omega_2 \rho^2}{4m_1 m_2} \middle| \begin{matrix} 1 - m_1, 1 - m_2 \\ 0, 0 \end{matrix} \right), \quad (50)$$

where $G[\cdot]$ is the Meijer's G-function [18]. Using [19, 07.23.26.0004.01], (50) can be expressed as

$$\mathbb{E}_{h_i} [J_0(h_i \rho)] = {}_2F_1 \left(m_1, m_2; 1; -\frac{\Omega_1 \Omega_2 \rho^2}{4m_1 m_2} \right), \quad (51)$$

where ${}_2F_1(\cdot, \cdot, \cdot, \cdot)$ is the Gauss hypergeometric function [18]. Using [19, 07.23.17.0046.01], the hypergeometric function can be expressed as a finite sum and (51) can be rewritten as

$$\mathbb{E}_{h_i} [J_0(h_i \rho)] = \frac{(m_1)_{m_2-1}}{(m_2-1)!} \sum_{k=0}^{m_1-1} \frac{(1-m_1)_k (1-m_2)_k}{(2-m_1-m_2)_k k!} \times \left(\frac{4m_1 m_2}{4m_1 m_1 + \Omega_1 \Omega_2 \rho^2} \right)^{m_1+m_2-k-1}. \quad (52)$$

Considering that all N vectors have the same m_1 , m_2 , Ω_1 and Ω_2 , using (47) and (52) and after some algebraic manipulations, the PDF of $|H|$ is given by

$$f_{|H|}(r) = r \left(\frac{(m_1)_{m_2-1}}{(m_2-1)!} \right)^N \sum_{k_1=0}^{m_1-1} \dots \sum_{k_N=0}^{m_1-1} \left(\frac{4m_1 m_2}{\Omega_1 \Omega_2} \right)^u \times \int_0^\infty \rho J_0(r \rho) \left(\frac{1}{\frac{4m_1 m_2}{\Omega_1 \Omega_2} + \rho^2} \right)^u d\rho. \quad (53)$$

It should be highlighted that $u \in \mathbb{Z}$, $u > 0$, since $m_1, m_2 \in \mathbb{Z}$. Utilizing [18, 6.565/4] in (53) and after some algebraic manipulations, (4) is derived and the proof is completed.

APPENDIX B PROOF OF (9)

Using L'Hospital's rule and [19, 03.04.20.0005.01], it stands that

$$\lim_{x \rightarrow 0} \frac{K_v(x)}{x^{-v}} = -\lim_{x \rightarrow 0} \frac{K_v(x)}{x^{-v}} + \lim_{x \rightarrow 0} \frac{x^{v+1}}{u} K_{v+1}(x). \quad (54)$$

Thus, the following expression stands

$$2v \lim_{x \rightarrow 0} x^v K_v(x) = \lim_{x \rightarrow 0} x^{v+1} K_{v+1}(x). \quad (55)$$

Using (55) and considering that $v \in \mathbb{Z}$, $v > 0$, the following expression can be derived

$$\lim_{x \rightarrow 0} x^v K_v(x) = 2^{v-1} (v-1)! \lim_{x \rightarrow 0} x K_1(x). \quad (56)$$

An approximation of $K_v(x)$ as $x \rightarrow 0$, if $\text{Re}\{v\} > 0$, where $\text{Re}\{\cdot\}$ denotes the real part of a complex number, is given by [27]

$$K_v(x) \simeq \frac{1}{2} \Gamma(v) \left(\frac{1}{2} x \right)^{-v}. \quad (57)$$

Hence, the following limit can be derived

$$\lim_{x \rightarrow 0} x K_1(x) = 1. \quad (58)$$

Utilizing (56) and (58), the proof is completed.

APPENDIX C PROOF OF PROPOSITION 9

To prove (40), $\mathbb{E}[\gamma_r^2]$ should be calculated, since $\mathbb{E}[\gamma_r]$ can be obtained from (23). The second moment of the received SNR can be obtained as

$$\mathbb{E}[\gamma_r^2] = l^2 \mathbb{E}[|H|^4] \gamma_t^2, \quad (59)$$

where $\mathbb{E}[|H|^4]$ can be derived as the fourth moment in (11), i.e.,

$$\mathbb{E}[|H|^4] = 2 \left(\frac{\Omega_1 \Omega_2}{m_1 m_2} \right)^2 \sum_{k_1=0}^{m_1-1} \dots \sum_{k_N=0}^{m_1-1} \prod_{i=1}^N \frac{(m_2)_{m_1-1-k_i} (1-m_2)_{k_i}}{(m_1-1-k)! k_i!} u(u+1). \quad (60)$$

Utilizing the proof of Proposition 5, (60) can be written as

$$\mathbb{E}[|H|^4] = 2 \left(\frac{\Omega_1 \Omega_2}{m_1 m_2} \right)^2 \sum_{k_1=0}^{m_1-1} \dots \sum_{k_N=0}^{m_1-1} \prod_{i=1}^N \frac{(m_2)_{m_1-1-k_i} (1-m_2)_{k_i}}{(m_1-1-k)! k_i!} u^2 - 2N \frac{\Omega_1^2 \Omega_2^2}{m_1 m_2}. \quad (61)$$

The first term in (61), termed as T , considering the definition of u can be written as

$$T_1 = 2 \sum_{k_1=0}^{m_1-1} \dots \sum_{k_N=0}^{m_1-1} \prod_{i=1}^N \frac{(m_2)_{m_1-1-k_i} (1-m_2)_{k_i}}{(m_1-1-k)! k_i!} \times \left((N(m_1+m_2-1))^2 - 2N(m_1+m_2-1) \sum_{i=1}^N k_i + \left(\sum_{i=1}^N k_i \right)^2 \right) \left(\frac{\Omega_1 \Omega_2}{m_1 m_2} \right)^2. \quad (62)$$

The first and the second term in (62) can be calculated utilizing the proof of Proposition 5. Using [19, 06.10.17.0002.02] and (27), it is proven that

$$k_i^2 (1-m_2)_{k_i} = (1-m_2) \left((2-m_2)(3-m_2)_{k_i} - (3-2m_2)(2-m_2)_{k_i} + (1-m_2)_{k_i} \right). \quad (63)$$

Using (26), (28) and (63), it can be proven that

$$\sum_{k_i=0}^{m_1-1} \frac{k_i^2 (m_2)_{m_1-1-k_i} (1-m_2)_{k_i}}{(m_1-1-k)! k_i!} = (1-m_2) \times \left((2-m_2) \frac{m_1(m_1+1)}{2} - (3-2m_2)m_1 + 1 - m_2 \right). \quad (64)$$

Utilizing (26), (28) and (64) and after some algebraic manipulations, the third term in (62), termed as T_2 , can be calculated as

$$T_2 = 2 \left(\frac{\Omega_1 \Omega_2}{m_1 m_2} \right)^2 N \left(\frac{(m_1-1)(m_2-1)}{2} (2-2m_2 + m_1(m_2-2)) + (N-1)((1-m_2)(m_1-1))^2 \right). \quad (65)$$

Using (65) and after some algebraic manipulations, (40) can be derived which completes the proof.

REFERENCES

- [1] S. Cherry, "Edholm's law of bandwidth," *IEEE Spectrum*, vol. 41, no. 7, pp. 58-60, Jul. 2004.

- [2] C. Pan, H. Ren, K. Wang, J. F. Kolb, M. ElKashlan, M. Chen, M. D. Renzo, Y. Hao, J. Wang, A. L. Swindlehurst, X. You, and L. Hanzo, "Reconfigurable Intelligent Surfaces for 6G and Beyond: Principles, Applications, and Research Directions," 2020. [Online]. Available: <https://arxiv.org/abs/2011.04300>
- [3] A. Yadav and O. A. Dobre, "All Technologies Work Together for Good: A Glance at Future Mobile Networks," *IEEE Wireless Commun.*, vol. 25, no. 4, pp. 10–16, Aug. 2018.
- [4] K. B. Letaief, W. Chen, Y. Shi, J. Zhang, and Y.-J. A. Zhang, "The Roadmap to 6G – AI Empowered Wireless Networks," 2019. [Online]. Available: <https://arxiv.org/abs/1904.11686>
- [5] E. Basar, M. Di Renzo, J. De Rosny, M. Debbah, M. Alouini, and R. Zhang, "Wireless Communications Through Reconfigurable Intelligent Surfaces," *IEEE Access*, vol. 7, pp. 116 753–116 773, Aug. 2019.
- [6] M. D. Renzo, M. Debbah, D.-T. Phan-Huy, A. Zappone, M.-S. Alouini, C. Yuen, V. Sciancalepore, G. C. Alexandropoulos, J. Hoydis, H. Gacanin, J. de Rosny, A. Bounceu, G. Lerosey, and M. Fink, "Smart Radio Environments Empowered by AI Reconfigurable Meta-Surfaces: An Idea Whose Time Has Come," 2019. [Online]. Available: <https://arxiv.org/abs/1903.08925>
- [7] I. Trigui, W. Ajib, and W.-P. Zhu, "A Comprehensive Study of Reconfigurable Intelligent Surfaces in Generalized Fading," 2020. [Online]. Available: <https://arxiv.org/abs/2004.02922>
- [8] Q. Wu and R. Zhang, "Intelligent Reflecting Surface Enhanced Wireless Network via Joint Active and Passive Beamforming," *IEEE Trans. Wireless Commun.*, vol. 18, no. 11, pp. 5394–5409, Nov. 2019.
- [9] Q. U. A. Nadeem, A. Kammoun, A. Chaaban, M. Debbah, and M. S. Alouini, "Asymptotic Max-Min SINR Analysis of Reconfigurable Intelligent Surface Assisted MISO Systems," *IEEE Trans. Wireless Commun.*, vol. 19, no. 12, pp. 7748–7764, Dec. 2020.
- [10] Z. Zhang, Y. Cui, F. Yang, and L. Ding, "Analysis and Optimization of Outage Probability in Multi-Intelligent Reflecting Surface-Assisted Systems," 2019. [Online]. Available: <https://arxiv.org/abs/1909.02193>
- [11] X. Qian, M. D. Renzo, J. Liu, A. Kammoun, and M.-S. Alouini, "Beamforming Through Reconfigurable Intelligent Surfaces in Single-User MIMO Systems: SNR Distribution and Scaling Laws in the Presence of Channel Fading and Phase Noise," 2020. [Online]. Available: <https://arxiv.org/abs/2005.07472>
- [12] V. D. Pegorara Souto, R. D. Souza, B. F. Uchôa-Filho, A. Li, and Y. Li, "Beamforming Optimization for Intelligent Reflecting Surfaces without CSI," *IEEE Wireless Commun. Lett.*, vol. 9, no. 9, pp. 1476–1480, Sept. 2020.
- [13] M. Badiu and J. P. Coon, "Communication Through a Large Reflecting Surface With Phase Errors," *IEEE Wireless Commun. Lett.*, vol. 9, no. 2, pp. 184–188, Feb. 2020.
- [14] M. H. Samuh and A. M. Salhab, "Performance Analysis of Reconfigurable Intelligent Surfaces over Nakagami-m Fading Channels," 2020. [Online]. Available: <https://arxiv.org/abs/2010.07841>
- [15] R. C. Ferreira, M. S. P. Facina, F. A. P. De Figueiredo, G. Fraidenraich, and E. R. De Lima, "Bit Error Probability for Large Intelligent Surfaces Under Double-Nakagami Fading Channels," *IEEE OJ-COMS*, vol. 1, pp. 750–759, May 2020.
- [16] I. Trigui, E. K. Agbogla, M. Benjillali, W. Ajib, and W.-P. Zhu, "Bit Error Rate Analysis for Reconfigurable Intelligent Surfaces with Phase Errors," 2021. [Online]. Available: <https://arxiv.org/abs/2101.03162>
- [17] G. K. Karagiannidis, N. C. Sagias, and P. T. Mathiopoulos, " N^* Nakagami: A Novel Stochastic Model for Cascaded Fading Channels," *IEEE Trans. Commun.*, vol. 55, no. 8, pp. 1453–1458, Aug. 2007.
- [18] I. S. Gradshteyn and I. M. Ryzhik, *Table of integrals, series, and products*. Academic press, 2014.
- [19] The Wolfram Functions Site [Online]. Available: <http://functions.wolfram.com>.
- [20] V. S. Adamchik and O. I. Marichev, "The algorithm for calculating integrals of hypergeometric type functions and its realization in reduce system," in *Proceedings of the International Symposium on Symbolic and Algebraic Computation*, ser. ISSAC '90, Tokyo, Japan, 1990, p. 212–224.
- [21] M. K. Simon and M.-S. Alouini, *Digital Communication over Fading Channels, 2nd Edition*. Wiley, 2004.
- [22] J. Lu, K. B. Letaief, J. C.-I. Chuang, and M. L. Liou, "M-PSK and M-QAM BER computation using signal-space concepts," *IEEE Trans. Commun.*, vol. 47, no. 2, pp. 181–184, Feb. 1999.
- [23] M. K. Simon and M.-S. Alouini, *Digital Communication over Fading Channels*. John Wiley & Sons, 2005.
- [24] O. S. Badarneh, P. C. Sofotasios, S. Muhaidat, S. L. Cotton, and D. B. Da Costa, "Product and Ratio of Product of Fisher-Snedecor F Variates and Their Applications to Performance Evaluations of Wireless Communication Systems," *IEEE Access*, vol. 8, pp. 215 267–215 286, Nov. 2020.
- [25] A. S. Lioumpas, G. K. Karagiannidis, and A. C. Iossifides, "Channel Quality Estimation Index (CQEI): A Long-Term Performance Metric for Fading Channels and an Application in EGC Receivers," *IEEE Trans. Wireless Commun.*, vol. 6, no. 9, pp. 3315–3323, Sep. 2007.
- [26] A. Abdi, H. Hashemi, and S. Nader-Esfahani, "On the PDF of the sum of random vectors," *IEEE Trans. Commun.*, vol. 48, no. 1, pp. 7–12, Jan. 2000.
- [27] M. Abramowitz and I. Stegun, *Handbook of Mathematical Functions: With Formulas, Graphs, and Mathematical Tables*, ser. Applied mathematics series. Dover Publications, 1965. [Online]. Available: <https://books.google.gr/books?id=MtU8uP7XMvoC>